



Association between exposure to different stone aggregates from asphalt and blood coagulability: A human exposure chamber study



Therese Bergh Nitter^{a,*}, Bjørn Hilt^{b,c}, Kristin v Hirsch Svendsen^a, Morten Buhagen^{b,c}, Rikke Bramming Jørgensen^a

^a Department of Industrial Economics and Technology Management, Norwegian University of Science and Technology (NTNU), Norway

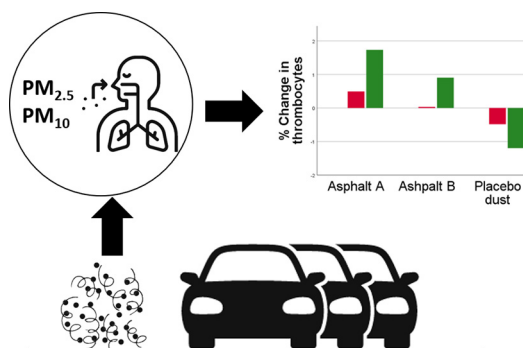
^b Department of Occupational Medicine, St. Olav's Hospital, Trondheim University Hospital, Trondheim, Norway

^c Department of Public Health and Nursing, NTNU, Norway

HIGHLIGHTS

- Road wear from asphalt is a significant contributor to local air pollution.
- Different types of asphalt have different blood coagulability potential.
- Coagulation potential and health outcome can be attributed to the chemical composition.
- Stone materials should be considered in the production of asphalt.

GRAPHICAL ABSTRACT



ARTICLE INFO

Article history:

Received 12 January 2021

Received in revised form 26 February 2021

Accepted 2 March 2021

Available online 8 March 2021

Editor: Lotfi Aleya

Keywords:

Blood coagulability

Stone aggregate

Non-exhaust emissions

Exposure chamber

Particulate matter

ABSTRACT

A large fraction of particulate matter (PM), especially PM₁₀, concentrations are due to non-exhaust emissions, such as road abrasion and wear on tires and brake pads. Concentrating on road abrasion, we aimed to investigate blood coagulability in healthy adults after exposure to two types of stone materials commonly used in asphalt on Norwegian roads.

This study followed a randomized, double-blind, cross-over study design. Using an exposure chamber, 24 healthy young volunteers were exposed to aggregates of two different types of rocks and placebo dust: quartz diorite, rhomb porphyry, and lactose (placebo dust). Each exposure session lasted for 4 hours (h), and blood samples were collected before exposure (baseline), 4 h post-exposure, and 24 h post-exposure to analyse potential changes in the von Willebrand factor (vWF) as well as of fibrinogen, d-dimer, leukocytes, and thrombocytes. The dust concentration in the exposure chamber was measured with real-time instruments and gravimetric samples of total dust, respirable dust, PM₁₀, PM_{2.5}, and ultrafine particles (UFP). The results were analysed using a linear mixed-effect model.

Leukocyte blood counts increased post-exposure for all exposure materials; however, none of the increases were statistically significant. The concentration of fibrinogen increased after exposure to quartz diorite, while it decreased after exposures to rhomb porphyry and lactose. Type of material was a statistically significant explanatory variable for the concentration of fibrinogen, with the most significant increase occurring 24 h post-exposure to quartz diorite. After exposure to the three materials, vWF decreased. For the thrombocytes, an increase in blood count was observed 24 h post-exposure to quartz diorite and rhomb porphyry, with a modest ($p = 0.09$) positive association for quartz diorite.

Abbreviations: ACH, Air change rate/air changes per hour; IL, Interleukin; PM, Particulate matter; vWFA, von Willebrand factor activity; vWFC, von Willebrand factor concentration.

* Corresponding author at: Alfred Getz veg 3, 7491, Trondheim, Norway

E-mail address: therese.nitter@ntnu.no (T.B. Nitter).

Although the results are limited, we conclude that the different effects observed post-exposure to quartz diorite support considering potential health effects when choosing materials in the production of asphalt.

© 2021 The Author(s). Published by Elsevier B.V. This is an open access article under the CC BY license (<http://creativecommons.org/licenses/by/4.0/>).

1. Introduction

Air pollution is a mixture of gases and particulate matter (PM), consisting of both organic and inorganic materials. Although all components found in the air are potentially harmful to human health, the most distinct health outcomes, such as asthma, cardiovascular diseases, lung cancer, and metabolic syndromes, have been attributed to exposure to PM (Cohen et al., 2018; Dockery et al., 1993; Franchini and Mannucci, 2011; Goldberg, 2008; Hoek et al., 2001; Kagawa, 2002). All of these outcomes are associated with inflammatory reactions (Xu et al., 2013).

PM is usually divided into PM_{10} , which consists of particles less than $10\ \mu\text{m}$ in aerodynamic diameter; $PM_{2.5}$, which consists of fine particles with aerodynamic diameters of less than $2.5\ \mu\text{m}$; and $PM_{0.1}$, which represents ultrafine particles (UFP) with aerodynamic diameters of less than $0.1\ \mu\text{m}$ (Brunekreef and Forsberg, 2005; World Health Organization, 2003). UFP tend to agglomerate through coagulation and condensation to form larger particles with diameters mainly between $0.1\ \mu\text{m}$ – $1.0\ \mu\text{m}$ (Brunekreef and Forsberg, 2005). Different size fractions tend to have particular chemical characteristics and deposit in specific locations along the respiratory tract (Heyder, 2004). In general, smaller particles are considered more toxic than larger particles due to their higher number concentrations, larger active surface areas, their ability to penetrate farther into the respiratory tract, and their propensity to react with more vulnerable cells and tissues (Delfino Ralph et al., 2005; Meng et al., 2013). Other results have, however, indicated that respiratory effects, such as chronic obstructive pulmonary disease and asthma, are more substantially or equally associated with short-term exposure to PM_{10} as compared to exposure to $PM_{2.5}$ (Brunekreef and Forsberg, 2005).

In urban areas, it is common to distinguish between exhaust and non-exhaust PM. While exhaust PM consists of particles released into the atmosphere from the combustion of gasoline or diesel oil, non-exhaust PM is produced from processes associated with vehicle usage and predominately comes from brakes linings, clutch pads, tires, and road surfaces (Thorpe and Harrison, 2008). Modern emission abatement technologies have provided a significant reduction in PM emissions from exhaust sources. Exhaust PM predominantly consists of $PM_{2.5}$ and is independent of weather and road conditions. PM from brakes and clutches consists of both $PM_{2.5}$ and PM_{10} . PM from the tire/road interface consists mainly of PM_{10} (Cassee et al., 2013; Garg et al., 2000; Ketzel et al., 2007) and is strongly dependent on weather and road conditions and on the use of studded tires. The non-exhaust sources remain a challenge, as they have received limited attention. The emissions from non-exhaust particles contribute up to 90% and 85% of the PM_{10} and $PM_{2.5}$ concentrations observed in urban areas, respectively (Bukowiecki et al., 2010; Ketzel et al., 2007; Timmers and Achten, 2016). If studded tires are used, it can be assumed that up to 90% of locally-emitted PM_{10} may be due to road abrasion during the winter (Johansson et al., 2007; Kupiainen et al., 2005).

The biological health effects associated with exposure to PM consist of oxidative stress reactions and inflammation, potentially resulting in deleterious cardiovascular and pulmonary health outcomes (Yang et al., 2017). To measure the health impact related to both short- and long-term exposure to PM, different biomarkers have been used in previous investigations. We must, however, realize that such markers are not entirely consistent, that they remain controversial, and that their specific biological significance in many cases remains unknown

(Elvidge et al., 2013; Yang et al., 2017). We often measure what we can measure but are not absolutely aware of whether changes in the different markers express pathological or physiological responses. Even so, the association between exposure to PM and health effects is well acknowledged.

1.1. Inflammation and blood clotting

Inflammation is a non-specific immune response in which the immune system acts to defend the body against xenobiotics. Inflammation plays an essential role in the initiation and development of atherosclerosis and the induction of cardiovascular events (Hajat et al., 2015). Acute inflammation is characterized by the infiltration of innate immune cells, specifically neutrophils and macrophages (Ferrero-Miliani et al., 2007). Neutrophils are recruited rapidly by the affected tissue in acute infections and dominate the initial influx of leukocytes (Issekutz and Movat, 1980). Later in the inflammation cycle, cytokines and reactive oxygen species are released to deal with foreign material and/or infected cells (Petrofsky and Bermudez, 1999). Cytokines are small, secreted proteins released by cells to communicate and interact with each other (Zhang and An, 2007).

Inflammation initiates blood clotting (Esmon, 2005), a physiological process involving components such as thrombocytes and proteins (Butenas, Mann, & Butenas, 2002). Blood clotting is characterized by an increased concentration in the acute-phase serum protein fibrinogen, which is then converted to insoluble fibrin, an essential ingredient in preventing infection from spreading into the bloodstream (Haidaris et al., 1989; Kattula et al., 2017). Hence, fibrin plays an essential role in thrombocyte aggregation and clot formation (Toss et al., 1997), and both fibrinogen and d-dimer are reckoned to be valid markers of blood coagulability. Another essential acute-phase protein is the von Willebrand factor (vWF) (A. D. Blann, 1991), which is a critical mediator of vascular inflammation. It plays a role in the recruitment of leukocytes and platelets in inflamed and injured tissue (Gragnano et al., 2017). Further, vWF is known to increase with stress and some diseases and conditions. To ensure stable blood clots (thrombus), the presence of both vWF and a network of fibrin is necessary (Kattula et al., 2017).

1.2. Materials used in asphalt

The type of asphalt laid on Norwegian roads depends on road use, both in terms of speed and daily traffic burden. Quartz and plagioclase are amongst the most dominant stone minerals used in Norwegian asphalt. Quartz is a hard mineral that is classified as a human carcinogen (International Agency for Research on Cancer, 1997; World Health Organization, 2000), and rock aggregates containing a high amount of quartz are considered more toxic to human health. In a Norwegian *in vitro* study, a strong negative correlation was found between the ability to induce inflammatory reactions in lung cells and the plagioclase content, and it was hypothesized that stone materials rich in plagioclase have low bioactivity (Øvrevik et al., 2005). Within this context, it is interesting to explore what effects the chemical and mineralogical compositions of particles in asphalt material may have on human health.

In this paper we aimed to investigate the formation of blood coagulation markers in healthy adults after exposure to different types of stone materials commonly used in asphalt on Norwegian roads.

2. Materials and methods

2.1. Study design

This study followed a randomized, double-blind, cross-over design, where the order and type of exposure were random for both volunteers and the researchers. For the study, we recruited 24 young volunteers. The experiment was carried out using six groups, each with four participants. Each person attended three dust exposure sessions in a chamber in random order: one with quartz diorite, one with rhomb porphyry, and one with lactose powder (placebo dust), which is an inert dust. At least 3 weeks passed between exposure sessions to eliminate hang-over effects. To increase their pulmonary ventilation during exposure in the exposure chamber, each participant used a step-board for 15 min during each exposure hour, achieving 50–75% of their maximum pulse. The strain was registered. During the remaining time, they sat by a table located in the middle of the room, where they could read, talk, or work on their phone/computer. The participants rotated through the seats around the table to reduce the variability in exposure related to the location in the room. The participants entered the exposure chamber in 30-minute intervals, in which the first participant was exposed for 4 h from 9 AM to 1 PM, and the last participant was exposed from 10:30 AM to 2:30 PM. The blinding was maintained until the statistical analysis commenced. The means and standard deviations of the chemical compositions of quartz diorite and rhomb porphyry are shown in Table 1. As shown in Table 1, quartz diorite and rhomb porphyry consisted predominantly of plagioclase while containing different quartz and chlorite contents.

These values are based on X-ray Diffraction (XDR) analyses of two crushing operations performed at different time points.

2.2. Study population

Twenty-four (10 men and 14 women) healthy, non-smoking volunteers (students) with normal lung function took part in the study. The ages of the volunteers ranged from 20 to 28 years. Before the volunteers were accepted as participants in this study, they were interviewed about respiratory health problems, chronic inflammatory diseases (such as rheumatism, ulcerous colitis, or Crohn's disease), sleep quality, and lifestyle. Candidates with any of these known illnesses or with symptoms thereof were excluded from the study. To maintain the anonymity of the volunteers, each participant was assigned an identification number (I.D.), which was used when information about the volunteers was recorded and stored. The volunteers were screened for lactose allergies before exposure. The lactose powder was inert and should not have been able to trigger any biological response in healthy subjects (VWR International, 2018).

Of the 24 subjects recruited, 23 completed all three exposure days. The participants were asked to avoid alcohol, specific nutrition, and challenging exercise for 36 h before each exposure day. The participants were also asked to achieve normal sleep and observe similar sleep patterns before each of the exposure days. On the days of exposure and before entering the exposure chamber, the participants were asked about symptoms related to colds and possible acute infections. Both during and after exposure, potential symptoms or irritations were registered using a standardized form. During the exposure, the participants used disposable overalls to prevent dermal exposure and their clothes from being contaminated. The participants received a modest remuneration

for each day of participation and a bonus for attending all three exposure days.

2.3. Inflammatory and coagulation parameters

Samples of blood were collected from the participants 30–60 min before the four-hour exposure session, 4 h after exposure ended, and again 24 h after exposure. Collection was done at two different locations, depending on the samples to be taken and tests to be done. The blood samples were collected in citrate plasma tubes. The tubes used for the d-dimer and fibrinogen analyses were stored at room temperature for a maximum of 8 h after sample collection. Prior to analysis, they were centrifugated at 2000 g for 10 min at 20 °C. The remaining citrate plasma tubes were centrifugated at 2500 g for 15 min at 20 °C within 30 min after sample collection and immediately stored at –20 °C. At the end of the day, all tubes were transported to the Laboratory of Clinical Biochemistry at St. Olav University Hospital in Trondheim, where they were analysed with accredited methods, as follows: i) Von Willebrand factor activity was measured via an immunoturbidimetric analysis, that is, monoclonal antibody to platelet binding sites on the von Willebrand factor (glycoprotein 1b receptor) were investigated (HemosIL von Willebrand Factor Activity Assay Kit); ii) fibrinogen was assessed via the optical detection of clots (HemosIL Q.F.A. Thrombin Assay Kit); iii) d-dimers were measured with a quantitative immunological method based on latex microparticles (HemosIL D-Dimer HS Assay Kit); and iv) leucocytes and thrombocytes were measured using a flowcytometric method (Sysmex XN Analyzer).

2.4. Dust exposure

The choice of aggregate types was based on previous in-vitro studies suggesting that plagioclase-rich rocks have a low potential to induce pro-inflammatory responses, while rocks containing minerals, such as quartz, amphibole, chlorite, and epidote, induced a marked increase in the release of IL-6 and IL-8 (Hetland et al., 2000; Øvrevik et al., 2005). In addition, quartz diorite and rhomb porphyry are also used in the asphalt of the largest, most-trafficked cities in Norway.

Both aggregates were produced using the standardized Los Angeles (LA) Method, which determines the resistance of an aggregate to fragmentation (European Committee for Standardisation 1998, EN 1097–2 annex A) to achieve a particle size of less than 65 µm. The quartz diorite has a ball mill value AN = 5,2 and LA value of 10,3, which means it can be used as a surface course on roads with annual average daily traffic (AADT) >15,000. The rhomb porphyry has a ball mill value AN = 7,5 and LA - value of 16,4, which means it can be used as a surface course on roads with AADT between 5000 and 15,000, according to existing requirements. The final size distributions and fractions of the two aggregates were analysed after crushing.

2.5. Exposure chamber

The exposure took place at the Department of Industrial Economics and Technology Management in the division of Health, Safety and Environmental Management at NTNU in Trondheim. The exposure chamber had an area of 11.8 m² and a volume of 35.0 m³. The air change rate (ACH) was 3.0 h⁻¹ during exposure to quartz diorite and rhomb porphyry. During exposure to lactose a lower ACH (2.06 h⁻¹) was used to increase the chamber exposure to this material. On 11 of the 19

Table 1

The means and standard deviations of the chemical compositions (%) of the two stone aggregates.

| Material | Quartz | K-feldspar | Plagioclase | Muscovite | Amphibole | Chlorite | Epidote | Calcium |
|----------------|------------|------------|-------------|-----------|-----------|------------|------------|-----------|
| Quartz diorite | 27.5 ± 0.7 | 12.0 ± 1.4 | 32.0 ± 1.4 | 3.0 ± 0.0 | | 10.5 ± 0.7 | 15.0 ± 0.0 | |
| Rhomb porphyry | 4.5 ± 0.7 | 31.0 ± 0.0 | 47.0 ± 0.0 | 7.0 ± 0.0 | 3.0 ± 0.0 | 5.5 ± 0.7 | | 2.0 ± 0.0 |

exposure days, the room temperature and relative humidity (RH) were measured. The mean temperature was 20.8 °C, while the temperature ranged from 18.1 to 23.1 °C, and the mean RH was 36%, with the RH ranging from 22 to 49%. Mixed ventilation was used, in which the air was supplied to the room by one air terminal located on the roof and extracted through two extract diffusers, also situated on the roof. To increase the mix of contaminants in the room, a table fan was placed near the closed window. The air used to generate the dust was filtered using HEPA filters before the exposure dust was supplied to the room to ensure that the generated particles were from the test material and not from outdoor pollution sources. Fig. 1 shows a sketch of the exposure chamber.

Aerosol generation was performed with a TSI 3410L Dust Aerosol Generator. The dust generator dispersed the dust into the facility through flexible silicone tubing that ended approximately 1.3 m above floor level in the middle of the wall. The walls and floor consisted of smooth surfaces that were easy to clean between each exposure session. To document that the chamber was adequately cleaned prior to dust generation, the particle concentration was measured (using DustTrack) at the beginning of each exposure session. In short, the feeding mass of a material (powder) is defined by the belt speed on the aerosol generator and the powder bulk density. For each of the materials, the dependency between the belt speed and feed mass was obtained (TSI Incorporated, 2018) so that the concentration, in mg/m³, could be calibrated to deliver a maximum of 10 mg/m³ of total dust and 5 mg/m³ of respirable dust, which correspond to the Norwegian eight-hour occupational exposure limit values for these particle fractions, respectively. The concentration was calculated based on the supplied air volume and mass balance for the exposure chamber (see Fig. 1). The photometric calibration factor (PCF) and the size calibration factor (SCF) in the calibration user settings were updated for each of the materials used. As a result, an individual calibration curve was created for each exposure material to achieve the wanted exposure concentrations. For lactose, a fluidized-bed Aerosol Generator 3400 (TSI) was used to disperse and aerosolize dry powders in a size range of 0.5 µm to 40 µm in aerodynamic diameter. The large beads in the fluidized-bed broke up the agglomerates of fine-powder particles.

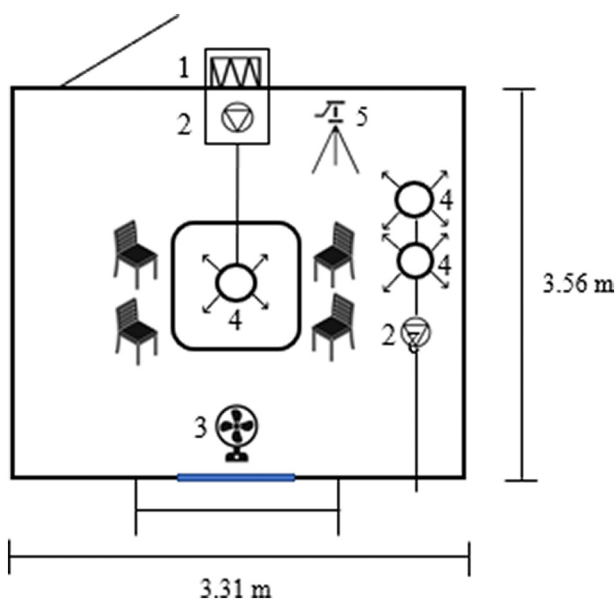


Fig. 1. The exposure chamber. Stationary samples were collected from the test stand, while personal samples were collected from each of the four people seated in the chamber. Symbols: 1 = air filter, 2 = pump, 3 = table fan, 4 = circular diffuser, 5 = test stand.

2.6. Exposure measurement

To measure and control the concentration of dust in the exposure chamber, both personal and stationary samples were collected, in addition to real-time measurements. To measure the variability in exposure between the subjects in the exposure chamber, personal samples of respirable particles were collected from each participant using a cyclone (SKC aluminium respirable cyclone) equipped with a cassette (SKC SureSeal 3-piece 37 mm) containing PCV filters (SKC PVC filter 37 mm 5.0 µm) connected to a sampling pump (SKC AirChek 3000). The sampling pump was calibrated to deliver a flow rate of 2.5 L/min for 4 h. The filters were weighed prior to and post exposure using a Mettler AE 163 scale (Mettler Instruments AG, Greifensee, Switzerland) with a limit of detection (LOD) of 0.05 mg. A reference filter was always weighed prior to weighing the experimental filters, and the standard deviation was calculated based on the average weight of the reference filter to obtain the LOD.

To obtain information about the temporal variability observed during each exposure day and to adjust the settings to obtain the desired exposure levels, real-time readings of PM₁, PM_{2.5}, PM₁₀, and respiratory dust fractions were obtained using DustTrak (TSI model DRX 8533) for the two stone types A and B and inert dust C. This instrument combines photometric measurements of the particle cloud and optical sizing of single particles in a unique visual system and measures different particle size fractions in the concentration range from 0.001 mg/m³ to 150 mg/m³ (Wang et al., 2009). The instrument is calibrated with standard ISO 12103-1 A1 test dust (Arizona road dust) from the factory.

For continuous measurement of UFP and submicron particles, a Scanning Mobility Particle Sizer (SMPS) was used (TSI Model 3938). Instrument use is described elsewhere (Jørgensen, 2019). The DRX 8355 and SMPS were located on the outside of the exposure chamber, with a plastic tube connected through the wall and fastened to a test stand on the inside of the exposure chamber for continuous monitoring.

Also attached to the test stand was equipment for taking stationary gravimetric samples of PM_{2.5} and recording respirable fractions, thoracic fractions, and "total dust". All gravimetric samples were collected on PVC filters (SKC 37 mm 5.0 µm). The sampling heads for PM_{2.5} (PEM™ 2.5 µm 2 l/min) and total dust (SKC SureSeal 37 mm 3-piece cassette) were each coupled to a pump (Casella Tuff personal air sampler) calibrated to deliver 2.0 L/min. For thoracic fraction sampling, a cyclone (BGI GK 2,69) with a cassette (SKC SureSeal 37 mm 3-piece cassette), calibrated to deliver a pump flow of 1.6 L/min, was used. For the stationary sampling of respirable dust, a cyclone (SKC aluminium respirable cyclone) equipped with a cassette (SKC SureSeal 37 mm 3 piece) connected to a pump (Casella Tuff personal air sampler), calibrated to deliver 2.5 L/min, was used. A verification of pump flow was done both prior to and after exposure. All filters were weighed before and after exposure, in the same room, next to the exposure chamber.

2.7. Statistical analysis

For descriptive statistics, concentrations were observed for each exposure material and for each exposure time, then analysed separately and checked for normality, as judged by the Shapiro-Wilk test and histograms. The results are shown in Table 3 and include arithmetic means and standard deviations (S.D.s).

The percent changes from baseline and to post exposure were calculated using the following formula:

$$\left(\left(\frac{\text{Post exposure}}{\text{Baseline}} \right) \times 100 \right) - 100$$

The percent change scores were not normally distributed, and for graphical illustration, data are presented as median values and their 95% confidence intervals (CIs). To analyse the absolute differences observed between the baseline scores (concentrations measured before

entering the exposure chamber) and those collected post exposure (4 h after exposure, and 24 h after exposure) for each exposure material, the paired *t*-test was used. For each of the parameters, one linear mixed-effect model was built. To estimate the trend for each exposure material (categorical variable), exposure time (categorical variable) and gender (categorical variable) these variables were interpreted as fixed effects, and the baseline score and birth year of the subjects were interpreted as a fixed covariates. I.D. was used as a subject variable, and a random intercept was included for each subject. When applying the linear mixed-effect model, we assumed that the same observations obtained from each subject were correlated and that the ones from different subjects were independent. It was also assumed that the residuals had a normal distribution with mean zero and constant variance. These assumptions were met after log transforming the values for fibrinogen and thrombocytes. For the remaining dependent variables, the distribution of the residuals was either symmetric (approximately normal) or slightly skewed, and the model assumption for the linear mixed-effects model was relaxed by using the Huber/White/Sandwich Estimator for the variance (robust linear mixed-effect model). After modelling the parameter estimates using the linear mixed-effect model, the Bonferroni post-hoc test was used for pairwise comparisons to determine whether the coagulation parameters differed between the different exposure materials. The results were analysed using STATA 15.

The study was approved by the Regional Ethics Committee (REK) (approval no.: 260381). All volunteers received detailed written and oral information concerning the study and signed a written consent document.

3. Results

The median concentrations of total dust, respiratory dust, PM_{2.5}, and UFP for each of the three exposure materials are shown in Table 2. The concentrations were lower for lactose compared to quartz diorite and rhomb porphyry. Lactose easily agglomerates and is a compact powder. While the aggregates from quartz diorite and rhomb porphyry are dry, lactose contains moisture, which makes it less disposable and difficult to achieve the same exposure concentrations as with quartz diorite and rhomb porphyry. Thus, a lower ACH was used in the exposure chamber for the dispersion of lactose.

The measured concentrations of coagulation markers are shown in Table 3. D-dimer assays were also performed. However, 93% of the samples collected were below the limit of quantification (0.3 µg/mL). Therefore, these data are not shown in Table 3 or used in the statistical analysis.

Table 2
Median and range concentrations for different particle size fractions measured during exposure.

| | Median | Range |
|--|--------|---------------|
| Quartz diorite | | |
| Thoracic dust (gravimetric) ^a mg/m ³ | 13.9 | 12.9–17.4 |
| Respirable dust (gravimetric) ^b mg/m ³ | 5.4 | 2.4–6.9 |
| PM _{2.5} (gravimetric) ^a mg/m ³ | 4.3 | 3.8–11.9 |
| UFP ^a (SMPS) | 1726.0 | 928.0–2782.0 |
| Rhomb porphyry | | |
| Thoracic dust (gravimetric) mg/m ³ | 16.8 | 11.8–20.6 |
| Respirable dust (gravimetric) mg/m ³ | 5.7 | 2.1–7.8 |
| PM _{2.5} (gravimetric) mg/m ³ | 5.1 | 3.8–15.5 |
| UFP (SMPS) | 2343.0 | 1832.0–7362.0 |
| Lactose | | |
| Thoracic dust (gravimetric) mg/m ³ | 2.5 | 1.0–4.6 |
| Respirable dust (gravimetric) mg/m ³ | 0.3 | 0.1–0.5 |
| PM _{2.5} (gravimetric) mg/m ³ | 1.2 | 0.8–5.4 |
| UFP (SMPS) | 678.0 | 202.0–1293.0 |

^a Stationary samples.

^b Personal samples.

As shown in Table 3, the concentration of fibrinogen increased at the 24 h post-exposure mark for quartz diorite. Post-exposure, the mean stayed the same for the lactose (although the SD increased). For B, the mean decreased, then increased again. Both vWFC and vWFA decreased post-exposure for all three exposure materials, but the decrease was most significant after exposure to quartz diorite, followed by rhomb porphyry. The leucocyte count increased post-exposure for all exposure materials. Thrombocytes increased 24 h post-exposure to quartz diorite and rhomb porphyry; however, they decreased post-exposure to lactose. The increase was most significant after exposure to quartz diorite.

The median percent changes in the outcome variables from baseline, along with their 95% confidence intervals, are shown in Fig. 2 for each of the three exposure materials. As shown in the figure, the percentage change in thrombocytes registered as an increase 24 h post-exposure to quartz diorite (1.92%) and rhomb porphyry (1.63%), while it registered as a decrease for lactose (−1.25%). According to the paired *t*-test, the difference between the absolute differences from baseline for quartz diorite and lactose 24 h post-exposure was of borderline statistical significance ($p = 0.06$). No statistical difference was observed between quartz diorite and rhomb porphyry or rhomb porphyry and lactose. According to the linear mixed-effect model, the highest concentrations of thrombocytes, after accounting for baseline and time, were observed post-exposure for quartz diorite ($p = 0.09$), followed by rhomb porphyry ($p = 0.039$). However, material as the fixed effect was not a significant explanatory factor for thrombocytes.

According to the linear mixed effect models, all coagulation markers occurred in lower concentrations in females compared to males, and for vWFA and vWFC, the differences in concentration between males and females reached statistical significance.

For fibrinogen, an increase of 3.12% was observed 24 h post-exposure to quartz diorite, while a decrease from baseline was observed post-exposure to rhomb porphyry and lactose. According to the paired *t*-test, the absolute changes between baseline and 4 h post-exposure and baseline and 24 h post-exposure were statistically significantly different when comparing the concentrations after exposure of quartz diorite and rhomb porphyry. The absolute changes were also statistically significantly different from baseline and 4-h post-exposure when comparing rhomb porphyry and lactose. The changes observed post-exposure to quartz diorite and lactose were not significantly different. According to the linear mixed-effect model, material was a significant explanatory variable for fibrinogen, after accounting for baseline values and time, a non-significant positive association was observed between fibrinogen and quartz diorite.

For vWFA and vWFC, decreases were observed from baseline and post-exposure for all exposure materials. The decrease was less significant post-exposure to lactose. Based on the linear mixed-effect model, type of material was not a significant explanatory variable for vWF.

Post-exposure, an increase in leukocytes was observed for all exposure materials, but according to the paired *t*-test, the only significant difference observed was between quartz diorite and lactose when comparing the changes from baseline and 24 h post-exposure ($p = 0.06$). According to the linear mixed-effect model, material was not a statistically significant fixed effect for the concentration of leukocytes. Based on Fig. 2, the median percent change was greater between baseline and 4-h post-exposure to lactose (19.4%), followed by quartz diorite (15.1%). However, 24 h post-exposure, a decrease was observed post-exposure to both quartz diorite and lactose, while an increase was observed post-exposure to rhomb porphyry.

In Table 4, the antilog values of the estimates of fixed effects (β) from the linear mixed-effect model are shown. To compare the three exposure materials, lactose is used as a reference and assigned a value of 1. For the thrombocytes, the estimate for quartz diorite is 1.02, while the estimates for rhomb porphyry and lactose are 1.01 and 1.0, respectively, meaning that the count for thrombocytes was higher post-exposure to quartz diorite, compared to rhomb porphyry and lactose. The estimate for quartz diorite is almost statistically significant ($p = 0.09$).

Table 3
Means and standard deviations of coagulation markers measured in blood.

| | Exposure to quartz diorite | | | Exposure to rhomb porphyry | | | Exposure to lactose | | |
|-----------------------------------|----------------------------|----------------------|-------------------------|----------------------------|----------------------|----------------------|----------------------|----------------------|----------------------|
| | Before ^a | 4 h after | 24 h after ^b | Before | 4 h after | 24 h after | Before | 4 h after | 24 h after |
| Thrombocyt ($\times 10^9/L$) | 268.6 (SD = 58.3) | 268.1 (SD = 57.3) | 272.3 (SD = 58.5) | 269.1 (SD = 61.8) | 265.3 (SD = 59.0) | 270.0 (SD = 56.3) | 272.6 (SD = 55.8) | 264.6 (SD = 52.4) | 269.8 (SD = 52.6) |
| Leukocyte ($\times 10^9/L$) | 5.6 (SD = 1.44) | 6.4 (SD = 1.6) | 6.2 (SD = 1.6) | 5.6 (SD = 1.5) | 6.6 (SD = 1.68) | 6.4 (SD = 1.6) | 5.7 (SD = 1.6) | 7.0 (SD = 1.9) | 6.1 (SD = 2.0) |
| Fibrinogen (g/l) | 2.4 (SD = 0.5) | 2.4 (SD = 0.5) | 2.51 (SD = 0.6) | 2.6 (SD = 0.6) | 2.4 (SD = 0.5) | 2.5 (SD = 0.5) | 2.4 (SD = 0.3) | 2.4 (SD = 0.4) | 2.4 (SD = 0.4) |
| vWfa ^c (IU/dl) | 105.4 (SD = 26.5) | 94.8 (SD = 24.2) | 98.7 (SD = 22.8) | 103.5 (SD = 25.8) | 93.5 (SD = 21.8) | 101.5 (SD = 25.3) | 105.0 (SD = 27.7) | 101.9 (SD = 24.7) | 106.1 (SD = 29.5) |
| vWfc ^d (IU/dl) | 118.6 (SD = 30.7) | 105.4 (SD = 25.7) | 109.7 (SD = 26.0) | 113.0 (SD = 25.5) | 107.9 (SD = 27.9) | 109.4 (SD = 24.0) | 116.8 (SD = 26.6) | 115.7 (SD = 25.8) | 116.9 (SD = 31.0) |

^a Before exposure (baseline).
^b The end of exposure.
^c von Willebrand factor activity.
^d von Willebrand concentration.

4. Discussion

The biological effects associated with exposure to PM are mainly oxidative stress and inflammation, both local and systemic, which can lead to both pulmonary and cardiovascular diseases. To assess the cardiovascular impact related to both short- and long-term exposure to PM, different biomarkers have been proposed in the literature. These markers, however, remain controversial, as they are not consistent (Yang et al., 2017). In this study, we measured the blood concentrations of inflammatory and coagulation parameters, namely, fibrinogen, leukocytes, vWfa, vWfc, and thrombocytes, pre- and post-exposure to two different exposure materials and one placebo.

Different types of environmental exposure chambers have been used to evaluate health effects from various exposures. In our exposure chamber, where the participants were exposed randomly for 4 h to each of the three materials, we were able to assure clean air before each exposure started and to keep the dust levels reasonably stable over time during and across the exposure days (Table 2). As the respiratory concentrations of quartz diorite and rhomb porphyry were almost identical, it is fair to assume that differences in biological response to these materials can be attributed to the differences in chemical composition and/or the surface activity/area of the particles.

The antilog of exposure estimates for the different coagulation markers was used to study the association between exposure material, time of sampling, and baseline readings. No other determinants were

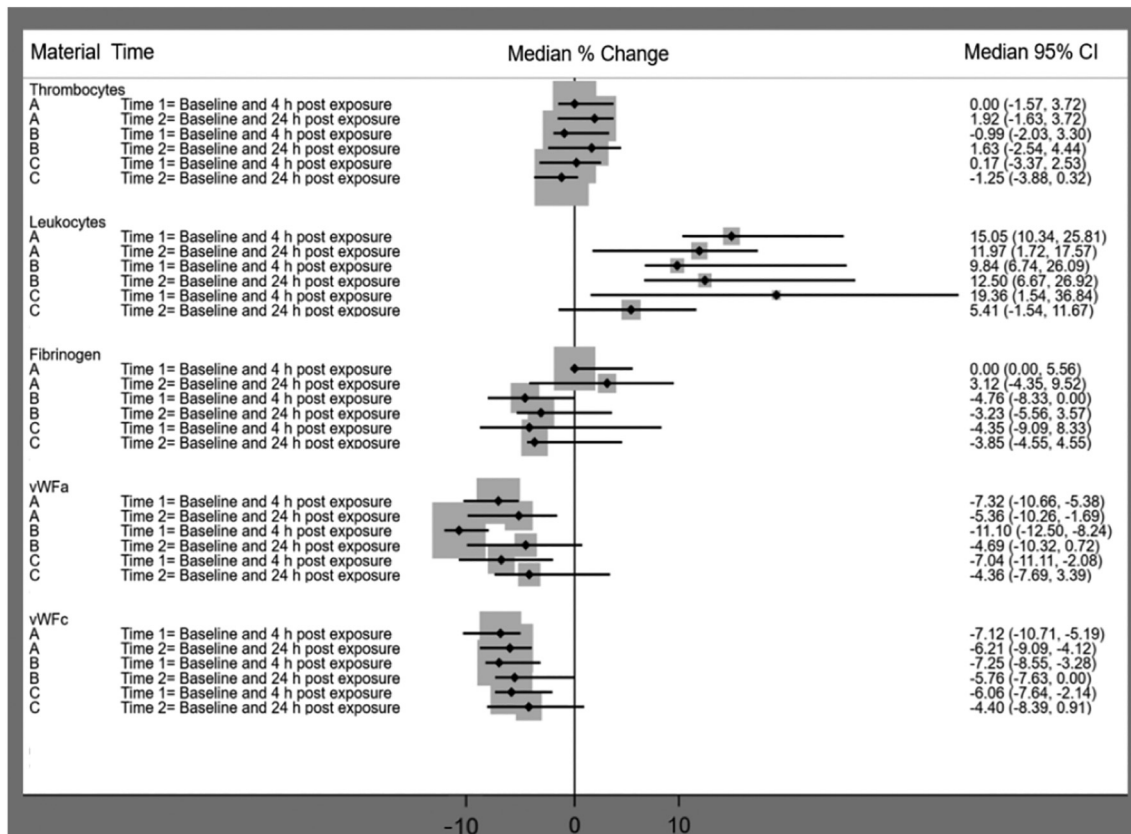


Fig. 2. Median % change from baseline for leukocytes, thrombocytes, fibrinogen, and vWF following exposure to quartz diorite (A), rhomb porphyry (B) and lactose (C).

Table 4

Antilog values for the mixed-effects model for the coagulation markers by exposure material, sampling time.

| Estimate | Fibrinogen | | | vWFa ^c | | | vWFc ^c | | | Leukocytes ^c | | | Thrombocytes | | |
|----------------|-------------------|--------|------|--------------------|--------|-------|--------------------|--------|-------|-------------------------|--------|------|-------------------------|--------|--------|
| | β | 95% CI | | β | 95% CI | | β | 95% CI | | β | 95% CI | | β | 95% CI | |
| Intercept | 1.06 | 0.96 | 1.18 | 44.77 ^b | 38.98 | 51.55 | 46.44 ^b | 39.01 | 55.15 | 3.25 ^b | 2.70 | 3.97 | 105.66 ^b | 99.20 | 112.54 |
| Material | | | | | | | | | | | | | | | |
| Quartz diorite | 1.01 | 0.98 | 1.04 | 0.97 | 0.92 | 1.24 | 0.95 ^a | 0.90 | 1.01 | 1.0 | 0.92 | 1.08 | 1.02^a | 1.0 | 1.03 |
| Rhomb porphyry | 0.97 ^b | 0.94 | 1.00 | 0.97 | 0.92 | 0.98 | 0.99 | 0.94 | 1.04 | 1.03 | 0.94 | 1.12 | 1.01 | 0.99 | 1.02 |
| Lactose | 1 | | | 1 | | | 1 | | | 1.0 | | | 1 | | |
| Time | | | | | | | | | | | | | | | |
| 1 | 0.98 ^b | 0.95 | 1.0 | 0.95 ^b | 0.92 | 0.97 | 0.97 ^b | 0.94 | 0.99 | 1.08 ^b | 1.04 | 1.12 | 0.99 | 0.98 | 1.01 |
| 2 | 1 | | | 1 | | | 1 | | | 1 | | | 1 | | |
| Gender | | | | | | | | | | | | | | | |
| Female | 0.99 | 0.94 | 1.05 | 0.94 ^b | 0.89 | 0.99 | 0.94 ^b | 0.91 | 0.98 | 0.96 | 0.85 | 1.09 | 0.98 | 0.95 | 1.01 |
| Male | 1 | | | 1 | | | 1 | | | 1 | | | 1 | | |
| Baseline | 1.40 ^b | 1.35 | 1.46 | 1.01 ^b | 1.01 | 1.01 | 1.01 ^b | 1.01 | 1.01 | 1.11 ^b | 1.07 | 1.15 | 1.03 ^b | 1.03 | 1.04 |

For Fibrinogen, material was a significant fixed effect.

Bold estimates show positive associations (values above 1), both significant as well as insignificant.

^a Significant at the 0.1 level.^b Significant at the 0.05 level.^c The residuals were slightly skewed, and the robust linear mixed-effect model was used for the parameter estimate.

used in the models, as each exposed subject was used as their own control, and exposure was done in random order.

Limited evidence was found for associations between coagulation markers and the three different types of dust. A small, non-significant positive association was found between quartz diorite and fibrinogen. A small but almost statistically significant ($p = 0.09$) association was also obtained between quartz diorite and the thrombocytes. A positive, non-significant association was also obtained between rhomb porphyry and thrombocytes and rhomb porphyry and leucocytes. To our knowledge, this is the first study in which coagulation markers have been measured pre- and post-exposure to different types of minerals used in asphalt, a significant contributor to non-exhaust air pollution.

Fibrinogen is a soluble plasma glycoprotein synthesized in the liver. An increased concentration of fibrinogen is considered a risk factor for cardiovascular events (Toss et al., 1997). According to the linear mixed-effect model for the concentration of fibrinogen, type of material, time, and baseline concentration were all statistically significant fixed effects. The patterns observed for the three exposure materials were different, as a decrease from baseline was observed post-exposure for rhomb porphyry and lactose, while an increase was observed for quartz diorite. The highest concentrations of fibrinogen were measured 24 h after exposure in the chamber. Using the Bonferroni post-hoc test for pairwise comparisons, a significant difference was observed between the two stone aggregates ($p = 0.02$), while there were no statistical differences between quartz diorite and lactose. Although the median percent change from baseline to post-exposure for lactose was significantly different from that for quartz diorite (see Fig. 1), the 95% CI for post-exposure to lactose was wide. Assumingly, for statistically significant results, more observations would be necessary.

Fibrinogen is one of the most used biomarkers for the risk of cardiovascular effects related to short- and long-term exposure to PM. The association between the two is, however, somehow controversial, as the results of some studies show an increase in the serum concentration of fibrinogen post-exposure to PM (Cozzi et al., 2007; Ghio et al., 2003; Hildebrandt et al., 2009; Hilt et al., 2002; S. Wu et al., 2014), while others have not found an association (Elvidge et al., 2013; Larsson et al., 2007; O'Toole et al., 2010). This inconsistency can be the result of different exposure concentrations and/or study designs. Another possible explanation may be the different responses to different chemical composition of particles, which could explain the difference in fibrinogen observed post-exposure to the three different exposure materials used in our study. Quartz diorite and rhomb porphyry

consisted of 27.5% and 4.0% quartz, respectively. In a recent study, a significant elevation of fibrinogen was observed amongst workers exposed to concentrations of quartz above 0.05 mg/m³ and between 0.03 mg/m³ and 0.05 mg/m³ (Westberg et al., 2019).

Now, vWF is known as a coagulation factor (glycoprotein) necessary for normal haemostasis and is considered to be a useful and sensitive marker of endothelial dysfunction (A. Blann, 1993; Spiel Alexander et al., 2008). Blood levels of vWF can be increased via endothelial cell damage (Horvath et al., 2004; Monroe Dougald and Hoffman, 2006) triggered by, for example, bacterial or virus infections and exposure to environmental pollutants (Abraham and Distler, 2007). In a recent meta-analysis of the association between PM and vWF, an elevation of 10 $\mu\text{g}/\text{m}^3$ of PM_{2.5} was associated with a 0.41% increase in vWF (Liang et al., 2020). However, in a review of 14 studies examining the association between exposure to PM and vWF, no association was found between short-term exposure and changes in vWF. In three out of six longitudinal studies, however, a significant association was found (Elvidge et al., 2013). As observed in our study, decreases in vWFa and vWFc were observed after exposure to all exposure materials. However, when accounting for time, baseline concentration, and type of material in the linear mixed-effect model, the lowest reduction was observed after exposure to lactose. Type of material as a fixed effect, however, failed to reach statistical significance. In a study of 38 men with chronic pulmonary diseases, a consistent decrease in vWF was observed for exposure to air pollutants 24 and 119 h post-exposure (Hildebrandt et al., 2009). In another study of a group of 40 healthy students exposed to air pollution in Beijing, a significant positive association was found between PM_{2.5}-PM₁₀ and vWF 4 days 6 days post-exposure (Shaowei Wu et al., 2012). In our study, decreases from baseline in vWFa and vWFc were observed 4 h post-exposure, while the concentrations rose again 20 h later. These results could indicate that, in order to study the change in vWF post-exposure to PM, samples have to be collected over a more extended period of time.

In a previous study, an elevation in thrombocyte aggregation was observed post-exposure to PM₁₀, which was seen a possible contributing factor to a higher incidence of cardiovascular events and mortality under certain given circumstances (Schicker et al., 2009). In our study, no change or a small decrease in the number of platelets was observed 4 h (early evening) post-exposure to the three exposure materials. We did, however, observe an increase 24 h post-exposure (noon/early afternoon) to both stone aggregates, with the most significant increase observed for quartz diorite ($p = 0.09$). This finding corresponds to the results of a previous

study, in which the highest thrombocyte counts were measured 24 h after subjects were exposed to PM (Cozzi et al., 2007).

A systemic inflammatory reaction, coupled with an increased number of leucocytes, is associated with pulmonary oxidative stress (Salvi et al., 1999). In two previous studies, a significant increase in leukocytes was observed with short-term exposure to PM₁₀ and diesel exhaust (Salvi et al., 1999; Schicker et al., 2009). In our study, a slight increase in leukocytes was observed post-exposure to all three exposure materials. Type of material as the fixed effect in the linear mixed-effect model was, however, not a statistically significant explanatory variable, as was the case when applying the post-hoc test and the paired *t*-test. There was, however, a difference in that the concentration decreased from 4 to 24 h post-exposure for quartz diorite and lactose, whereas the concentration continued to increase 24 h post-exposure for rhomb porphyry (see Fig. 1).

Some in vitro studies have been conducted to study the biological relevance of the chemical composition of PM. In one study, rat lung alveolar macrophages and alveolar type 2 cells were exposed for 20 h in vitro to different stone particles (mylonite, feldspar, gabbro, and quartz). The mylonite used in this study is similar to the quartz diorite used in our study. The release of the inflammatory cytokines interleukin-6 (IL-6), TNF- α , and macrophage inflammatory protein-2 (MIP-2) were measured. Dust from mylonite was found to be the most potent exposure dust, followed by gabbro. Both gabbro and mylonite contain epidote and chlorite. Mylonite also contains quartz (Becher et al., 2001). Gabbro contains a high amount of amphibole, which is a fibrous mineral with some similarities to asbestos associated with the potency observed after exposure to gabbro dust (Becher et al., 2001). In another in vitro study, A549 cells were exposed for 40 h to different types of mineral particles (mylonite, gabbro, basalt, and feldspar) at concentrations between 0 and 100 $\mu\text{g}/\text{cm}^2$. All particles induced increases in IL-6 and IL-8 with increasing particle concentration, but the potencies of the different materials varied widely. In correspondence with previous findings, mylonite was found to be the most potent dust, which can be explained by a high quartz content combined with chlorite/epidote. Gabbro did not contain quartz but did contain 35% amphibole. Feldspar (99% plagioclase) did not show any significant cytotoxic effects at any level of exposure (Hetland et al., 2000).

In a recent study, conducted at the National Institute of Public Health in Norway, the pro-inflammatory cytokine response (IL-8, IL-1 β , IL-1 α , and TNF α) was tested for two different types of cells. Bronchial epithelial cells (HBEC3-KT) and cells similar to the immune cells in the macrophages (THP-1 cells) were exposed to six different rock samples, including rhomb porphyry and quartz diorite. The results showed that the two stone aggregates were not the most potent of the rock samples in any of the cell types, but that quartz diorite was significantly more potent than rhomb porphyry in inducing IL-8 and TNF α in the THP-1 cells. For the HBEC3-KT cells no significant differences were observed between quartz diorite and rhomb porphyry for any of the cytokines (Grytting et al., 2021; Erichsen et al., 2020).

Although other inflammatory markers of health effects were used in these in vitro studies, the results obtained are similar to the findings of our study. It should, however, be noted that, based on previous findings, it is difficult to conclude whether it is single minerals causing the changes in observed inflammatory markers or the composition of the material as a whole.

Compared to in vitro studies, controlled exposure in humans is the most powerful method for testing hypotheses related to the biological responses occurring during and after exposure to xenobiotics (Seagrave et al., 2005). However, the main drawback of human exposure studies is the often-limited number of participants and their heterogeneity. As it is not likely that all subjects will respond in the same manner to exposure, reaching statistical significance after short-term exposure on a limited number of subjects is often challenging. Even so, we think that our results have provided some new knowledge that can be tested in future studies.

5. Conclusions

These results contribute to our knowledge of the health effects of exposure to non-exhaust emissions with differing chemical compositions. Despite a limited association observed towards a higher coagulability, an almost statistically significant ($p = 0.09$) association was observed between exposure to quartz diorite and the count of thrombocytes. In addition, a positive non-significant relationship was observed for fibrinogen, also post exposure to quartz diorite, and the differences observed post-exposure to quartz diorite and rhomb porphyry were statistically significant ($p = 0.02$). Although the associations are weak, the effect observed post-exposure to quartz diorite supports considering potential health effects when choosing stone materials in the production of asphalt.

Funding

This research received funding from the The Research Council of Norway and is a part of a larger project called "Preventive measures to reduce the adverse health impact of traffic-related air pollution (PreventTAP)". PreventTAP includes several different partners and is led by the Norwegian Institute of Public Health.

CRedit authorship contribution statement

The work presented in this article has been ongoing since the beginning of 2017, and all authors have contributed to the work in significant ways. This project is funded by the Norwegian Research Council and conducted by the Norwegian University of Science and Technology (NTNU). In this author statement, the individual contributions from the five authors are stated using the relevant CRedit roles.

In collaboration, certified occupational hygienist and Professor Rikke Bramming Jørgensen, Professor Bjørn Hilt, certified occupational hygienist and Professor Kristin v Hirsch Svendsen, and chemist and certified occupational hygienist Morten Buhagen have participated in the conceptualization process, designing the methodology, provision of study materials (resources), and rewriting and editing the draft submitted to the journal. Dr. Therese Bergh Nitter (corresponding author) has been responsible for performing the formal analysis using STATA, validating the results and calculations, writing, rewriting, and editing the draft submitted to the journal.

Declaration of competing interest

The authors have no conflicts of interest to declare.

Acknowledgements

The authors would like to thank Eyolf Erichsen and Torkil S. Røhr at the Geological Survey of Norway for performing the XRD analysis of the two stone aggregates used. The authors would also like to acknowledge the contributions from Liv Bjerke Rodal from the Department of Occupational Medicine, St. Olav's Hospital, and Kirsti Sørås, Guro Almvik, Anne Risdal, and Gøril Bakken from the Clinical Research Facility at St. Olav's Hospital, Trondheim University Hospital. Finally, these acknowledgements would not be complete without mentioning Arne Vidar Sjøenst and Siri Fenstad Ragde.

References

- Abraham, D., Distler, O., 2007. How does endothelial cell injury start? The role of endothelin in systemic sclerosis. *Arthritis Research & Therapy* 2 (Suppl. 2). https://doi.org/10.1186/ar2186_9_Suppl_S2-S2.
- Becher, R., Hetland, R.B., Refsnes, M., Dahl, J.E., Dahlman, H.J., Schwarze, P.E., 2001. Rat lung inflammatory responses after in vivo and in vitro exposure to various stone particles. *Inhal. Toxicol.* 13 (9), 789–805. <https://doi.org/10.1080/08958370118221>.
- Blann, A., 1993. von Willebrand factor and the endothelium in vascular disease. *Br. J. Biomed. Sci.* 50 (2), 125–134.

- Blann, A.D., 1991. von Willebrand factor antigen as an acute phase reactant and marker of endothelial cell injury in connective tissue diseases: a comparison with CRP, rheumatoid factor, and erythrocyte sedimentation rate. *Z. Rheumatol.* 50 (5), 320–322.
- Brunekreef, B., Forsberg, B., 2005. Epidemiological evidence of effects of coarse airborne particles on health. *Eur. Respir. J.* 26 (2), 309–318. <https://doi.org/10.1183/09031936.05.00001805>.
- Bukowiecki, N., Lienemann, P., Hill, M., Furger, M., Richard, A., Amato, F., ... Gehrig, R., 2010. PM10 emission factors for non-exhaust particles generated by road traffic in an urban street canyon and along a freeway in Switzerland. *Atmos. Environ.* 44 (19), 2330–2340. <https://doi.org/10.1016/j.atmosenv.2010.03.039>.
- Butenas, S., Mann, K.G., Butenas, 2002. Blood coagulation. *Biochem. Mosc.* 67 (1), 3–12. <https://doi.org/10.1023/A:1013985911759>.
- Cassee, F.R., Héroux, M.-E., Gerlofs-Nijland, M.E., Kelly, F.J., 2013. Particulate matter beyond mass: recent health evidence on the role of fractions, chemical constituents and sources of emission. *Inhal. Toxicol.* 25 (14), 802–812. <https://doi.org/10.3109/08958378.2013.850127>.
- Cohen, G., Levy, I., Yuval, Kark, J.D., Levin, N., Witberg, G., ... Gerber, Y., 2018. Chronic exposure to traffic-related air pollution and cancer incidence among 10,000 patients undergoing percutaneous coronary interventions: a historical prospective study. *Eur. J. Prev. Cardiol.* 25 (6), 659–670. <https://doi.org/10.1177/2047487318760892>.
- Cozzi, E., Wingard, C.J., Cascio, W.E., Devlin, R.B., Miles, J.J., Boffending, A.R., ... Henriksen, R.A., 2007. Effect of ambient particulate matter exposure on hemostasis. *Transl. Res.* 149 (6), 234–232.
- Delfino Ralph, J., Sioutas, C., Malik, S., 2005. Potential role of ultrafine particles in associations between airborne particle mass and cardiovascular health. *Environ. Health Perspect.* 113 (8), 934–946. <https://doi.org/10.1289/ehp.7938>.
- Dockery, D.W., Pope, C.A., Xu, X., Spengler, J.D., Ware, J.H., Fay, M.E., ... Speizer, F.E., 1993. An association between air pollution and mortality in six U.S. cities. *N. Engl. J. Med.* 329 (24), 1753–1759. <https://doi.org/10.1056/NEJM199312093292401>.
- Elvidge, T., Matthews, I.P., Gregory, C., Hoogendoorn, B., 2013. Feasibility of using biomarkers in blood serum as markers of effect following exposure of the lungs to particulate matter air pollution. *Journal of Environmental Science and Health, Part C* 31 (1), 1–44. <https://doi.org/10.1080/10590501.2013.763575>.
- Erichsen, E., Grytting, V.S., Røhr, T.R., Halle, M.S., Ulvik, A., Pettersen, E., ... Van der Lelij, R., 2020. Karakterisering av partikler fra mineral- og bergartsprøver for bruk i studier av betennelsesreaksjoner i celleprøver. Retrieved from. <https://hdl.handle.net/11250/2678243>.
- Esmon, C.T., 2005. The interactions between inflammation and coagulation. *Br. J. Haematol.* 131 (4), 417–430. <https://doi.org/10.1111/j.1365-2141.2005.05753.x>.
- Ferrero-Miliani, L., Nielsen, O.H., Andersen, P.S., Girardin, S.E., 2007. Chronic inflammation: importance of NOD2 and NALP3 in interleukin-1beta generation. *Clin. Exp. Immunol.* 147 (2), 227–235. <https://doi.org/10.1111/j.1365-2249.2006.03261.x>.
- Franchini, M., Mannucci, P.M., 2011. Thrombogenicity and cardiovascular effects of ambient air pollution. *Blood* 118 (9), 2405–2412. <https://doi.org/10.1182/blood-2011-04-343111>.
- Garg, B.D., Cadle, S.H., Mulawa, P.A., Groblicki, P.J., Laroo, C., Parr, G.A., 2000. Brake wear particulate matter emissions. *Environ. Sci. Technol.* 34 (21), 4463–4469. <https://doi.org/10.1021/es001108h>.
- Ghio, A.J., Hall, A., Bassett, M.A., Cascio, W.E., Devlin, R.B., 2003. Exposure to concentrated ambient air particles alters hematologic indices in humans. *Inhal. Toxicol.* 15 (14), 1465–1478. <https://doi.org/10.1080/08958370390249111>.
- Goldberg, M., 2008. A systematic review of the relation between long-term exposure to ambient air pollution and chronic diseases. *Rev. Environ. Health* 23 (4), 243–298. <https://doi.org/10.1515/REVEH.2008.23.4.243>.
- Gragano, F., Sperlongano, S., Golia, E., Natale, F., Bianchi, R., Crisci, M., ... Calabrò, P., 2017. The role of von Willebrand factor in vascular inflammation: from pathogenesis to targeted therapy. *Mediat. Inflamm.* 2017, 5620314. <https://doi.org/10.1155/2017/5620314>.
- Grytting, V.S., Refsnes, M., Øvrevik, J., Halle, M., Schönenberger, J., Lelij, R.v., ... Låg, M., 2021. Respirable stone particles differ in their ability to induce cytotoxicity and pro-inflammatory responses in cell models of the human airways. *Particle Fiber and Toxicology* This manuscript is under review (second revision).
- Haidaris, P.J., Francis, C.W., Sporn, L.A., Arvan, D.S., Collichio, F.A., Marder, V.J., 1989. Megakaryocyte and hepatocyte origins of human fibrinogen biosynthesis exhibit hepatocyte-specific expression of gamma chain-variant polypeptides. *Blood* 74 (2), 743–750.
- Hajat, A., Allison, M., Diez-Roux, A.V., Jenny, N.S., Jorgensen, N.W., Szpiro, A.A., ... Kaufman, J.D., 2015. Long-term exposure to air pollution and markers of inflammation, coagulation, and endothelial activation: a repeat-measures analysis in the Multi-Ethnic Study of Atherosclerosis (MESA). *Epidemiology (Cambridge, Mass.)* 26 (3), 310–320. <https://doi.org/10.1097/EDE.0000000000000267>.
- Hetland, R.B., Refsnes, M., Myran, T., Johansen, B.V., Uthus, N., Schwarze, P.E., 2000. Mineral and/or metal content as critical determinants of particle-induced release of il-6 and il-8 from A549 cells. *J. Toxic. Environ. Health A* 60 (1), 47–65. <https://doi.org/10.1080/009841000156583>.
- Heyder, J., 2004. Deposition of inhaled particles in the human respiratory tract and consequences for regional targeting in respiratory drug delivery. *Proc. Am. Thorac. Soc.* 1 (4), 315–320. <https://doi.org/10.1513/pats.200409-046TA>.
- Hildebrandt, K., Rückel, R., Koenig, W., Schneider, A., Pitz, M., Heinrich, J., ... Peters, A., 2009. Short-term effects of air pollution: a panel study of blood markers in patients with chronic pulmonary disease. *Particle and Fibre Toxicology* 6, 25. <https://doi.org/10.1186/1743-8977-6-25>.
- Hilt, B., Qvenild, T., Holme, J., Svendsen, K., Ulvestad, B., 2002. Increase in interleukin-6 and fibrinogen after exposure to dust in tunnel construction workers. *Occup. Environ. Med.* 59 (1), 9–12. <https://doi.org/10.1136/oem.59.1.9>.
- Hoek, G., Brunekreef, B., Fischer, P., van Wijnen, J., 2001. The association between air pollution and heart failure, arrhythmia, embolism, thrombosis, and other cardiovascular causes of death in a time series study. *Epidemiology* 12 (3), 355–357.
- Horvath, B., Hegedus, D., Szapary, L., Marton, Z., Alexy, T., Koltai, K., ... Kesmarky, G., 2004. Measurement of von Willebrand factor as the marker of endothelial dysfunction in vascular diseases. *Exp. Clin. Cardiol.* 9 (1), 31–34.
- International Agency for Research on Cancer, 1997. *Monographs on the evaluation of carcinogenic risks to humans. Silica, Some Silicates, Coal Dust and para-Aramid Fibrils.* Vol. 68 (Vol. 68).
- Issekutz, A.C., Movat, H.Z., 1980. The in vivo quantitation and kinetics of rabbit neutrophil leukocyte accumulation in the skin in response to chemotactic agents and *Escherichia coli*. *Lab. Invest.* 42 (3), 310–317.
- Johansson, C., Norman, M., Gidhagen, L., 2007. Spatial & temporal variations of PM10 and particle number concentrations in urban air. *Environ. Monit. Assess.* 127 (1), 477–487. <https://doi.org/10.1007/s10661-006-9296-4>.
- Jørgensen, R.B., 2019. Comparison of four nanoparticle monitoring instruments relevant for occupational hygiene applications. *Journal of Occupational Medicine and Toxicology* 14 (1), 28. <https://doi.org/10.1186/s12995-019-0247-8>.
- Kagawa, J., 2002. Health effects of diesel exhaust emissions—a mixture of air pollutants of worldwide concern. *Toxicology* 181–182, 349–353. [https://doi.org/10.1016/S0300-483X\(02\)00461-4](https://doi.org/10.1016/S0300-483X(02)00461-4).
- Kattula, S., Byrnes, J.R., Wolberg, A.S., 2017. Fibrinogen and fibrin in hemostasis and thrombosis. *Arterioscler. Thromb. Vasc. Biol.* 37 (3), e13–e21. <https://doi.org/10.1161/ATVBAHA.117.308564>.
- Ketzel, M., Omstedt, G., Johansson, C., Düring, I., Pohjola, M., Oettl, D., ... Berkowicz, R., 2007. Estimation and validation of PM2.5/PM10 exhaust and non-exhaust emission factors for practical street pollution modelling. *Atmos. Environ.* 41 (40), 9370–9385. <https://doi.org/10.1016/j.atmosenv.2007.09.005>.
- Kupiainen, K.J., Tervahattu, H., Räisänen, M., Mäkelä, T., Aurela, M., Hillamo, R., 2005. Size and composition of airborne particles from pavement wear, tires, and traction sanding. *Environ. Sci. Technol.* 39 (3), 699–706. <https://doi.org/10.1021/es035419e>.
- Larsson, B.M., Sehlstedt, M., Grunewald, J., Sköld, C.M., Lundin, A., Blomberg, A., ... Svartengren, M., 2007. Road tunnel air pollution induces bronchoalveolar inflammation in healthy subjects. *Eur. Respir. J.* 29 (4), 699. <https://doi.org/10.1183/09031936.00035706>.
- Liang, Q., Sun, M., Wang, F., Ma, Y., Lin, L., Li, T., ... Sun, Z., 2020. Short-term PM(2.5) exposure and circulating von Willebrand factor level: a meta-analysis. *Sci. Total Environ.* 737, 140180. <https://doi.org/10.1016/j.scitotenv.2020.140180>.
- Meng, X., Ma, Y., Chen, R., Zhou, Z., Chen, B., Kan, H., 2013. Size-fractionated particle number concentrations and daily mortality in a Chinese city. *Environ. Health Perspect.* 121 (10), 1174–1178. <https://doi.org/10.1289/ehp.1206398>.
- Monroe Douglas, M., Hoffman, M., 2006. What does it take to make the perfect clot? *Arterioscler. Thromb. Vasc. Biol.* 26 (1), 41–48. <https://doi.org/10.1161/01.ATV.0000193624.28251.83>.
- O'Toole, T.E., Hellmann, J., Wheat, L., Haberzettl, P., Lee, J., Conklin, D.J., ... Pope 3rd, C.A., 2010. Episodic exposure to fine particulate air pollution decreases circulating levels of endothelial progenitor cells. *Circ. Res.* 107 (2), 200–203. <https://doi.org/10.1161/CIRCRESAHA.110.222679>.
- Øvrevik, J., Myran, T., Refsnes, M., Låg, M., Becher, R., Hetland, R.B., Schwarze, P.E., 2005. Mineral particles of varying composition induce differential chemokine release from epithelial lung cells: importance of physico-chemical characteristics. *The Annals of Occupational Hygiene* 49 (3), 219–231. <https://doi.org/10.1093/annhyg/meh087>.
- Petrofsky, M., Bermudez, L.E., 1999. Neutrophils from *Mycobacterium avium*-infected mice produce TNF- α , IL-12, and IL-1 β and have a putative role in early host response. *Clin. Immunol.* 91 (3), 354–358. <https://doi.org/10.1006/clim.1999.4709>.
- Salvi, S., Blomberg, A., Rudell, B., Kelly, F., Sandström, T., Holgate, S.T., Frew, A., 1999. Acute inflammatory responses in the airways and peripheral blood after short-term exposure to diesel exhaust in healthy human volunteers. *Am. J. Respir. Crit. Care Med.* 159 (3), 702–709. <https://doi.org/10.1164/ajrccm.159.3.9709083>.
- Schicker, B., Kuhn, M., Fehr, R., Asmis, L.M., Karagiannidis, C., Reinhart, W.H., 2009. Particulate matter inhalation during hay storing activity induces systemic inflammation and platelet aggregation. *Eur. J. Appl. Physiol.* 105 (5), 771–778. <https://doi.org/10.1007/s00421-008-0962-9>.
- Seagrave, J., McDonald, J.D., Mauderly, J.L., 2005. In vitro versus in vivo exposure to combustion emissions. *Exp. Toxicol. Pathol.* 57, 233–238. <https://doi.org/10.1016/j.etp.2005.05.011>.
- Spiel Alexander, O., Gilbert James, C., Jilma, B., 2008. Von Willebrand factor in cardiovascular disease. *Circulation* 117 (11), 1449–1459. <https://doi.org/10.1161/CIRCULATIONAHA.107.722827>.
- Thorpe, A., Harrison, R.M., 2008. Sources and properties of non-exhaust particulate matter from road traffic: a review. *Sci. Total Environ.* 400 (1), 270–282. <https://doi.org/10.1016/j.scitotenv.2008.06.007>.
- Timmers, V.R.J.H., Achten, P.A.J., 2016. Non-exhaust PM emissions from electric vehicles. *Atmos. Environ.* 134, 10–17. <https://doi.org/10.1016/j.atmosenv.2016.03.017>.
- Toss, H., Lindahl, B., Siegbahn, A., Wallentin, L., 1997. Prognostic influence of increased fibrinogen and C-reactive protein levels in unstable coronary artery disease. FRISC Study Group. *Fragmin during instability in coronary artery disease. Circulation* 96 (12), 4204–4210. <https://doi.org/10.1161/01.cir.96.12.4204>.
- TSI Incorporated, 2018. *Dust Aerosol Generator Model 3410L In.*
- VWR International, 2018. *Safety Sheet CAS-nr.: 10039-26-6.*
- Wang, X., Chancellor, G., Evenstad, J., Farnsworth, J.E., Hase, A., Olson, G.M., ... Agarwal, J.K., 2009. A novel optical instrument for estimating size segregated aerosol mass concentration in real time. *Aerosol Sci. Technol.* 43 (9), 939–950. <https://doi.org/10.1080/02786820903045141>.
- Westberg, H., Hedbrant, A., Persson, A., Bryngelsson, I.-L., Johansson, A., Ericsson, A., ... Andersson, L., 2019. Inflammatory and coagulatory markers and exposure to different

- size fractions of particle mass, number and surface area air concentrations in Swedish iron foundries, in particular respirable quartz. *Int. Arch. Occup. Environ. Health* 92 (8), 1087–1098. <https://doi.org/10.1007/s00420-019-01446-z>.
- World Health Organization, 2000. Crystalline Silica, Quartz. 24 Retrieved from. <https://www.who.int/ipcs/publications/cicad/en/cicad24.pdf>.
- World Health Organization, 2003. Health Aspects of Air Pollution with Particulate Matter, Ozone and Nitrogen Dioxide. Retrieved from. https://www.euro.who.int/__data/assets/pdf_file/0005/112199/E79097.pdf.
- Wu, S., Deng, F., Wei, H., Huang, J., Wang, H., Shima, M., ... Guo, X., 2012. Chemical constituents of ambient particulate air pollution and biomarkers of inflammation, coagulation and homocysteine in healthy adults: a prospective panel study. *Particle and Fibre Toxicology* 9 (1), 49. <https://doi.org/10.1186/1743-8977-9-49>.
- Wu, S., Deng, F., Wei, H., Huang, J., Wang, X., Hao, Y., ... Guo, X., 2014. Association of cardiopulmonary health effects with source-appointed ambient fine particulate in Beijing, China: a combined analysis from the Healthy Volunteer Natural Relocation (HVNR) study. *Environ. Sci. Technol.* 48 (6), 3438–3448. <https://doi.org/10.1021/es404778w>.
- Xu, X., Jiang, S.Y., Wang, T.-Y., Bai, Y., Zhong, M., Wang, A., ... Sun, Q., 2013. Inflammatory response to fine particulate air pollution exposure: neutrophil versus monocyte. *PLoS One* 8 (8), e71414. <https://doi.org/10.1371/journal.pone.0071414>.
- Yang, L., Hou, X.-Y., Wei, Y., Thai, P., Chai, F., 2017. Biomarkers of the health outcomes associated with ambient particulate matter exposure. *Sci. Total Environ.* 579, 1446–1459. <https://doi.org/10.1016/j.scitotenv.2016.11.146>.
- Zhang, J.-M., An, J., 2007. Cytokines, inflammation, and pain. *Int. Anesthesiol. Clin.* 45 (2), 27–37. <https://doi.org/10.1097/AIA.0b013e318034194e>.